Evaluating the Microwave Performance of Epidermal Electronics with Equivalent Transmission Line Modeling

Tammy Chang[1,2], Jonathan A. Fan[2], and Thomas H. Lee[1]
[1]Stanford Microwave Integrated Circuits Laboratory, Stanford University, Stanford, CA 94305
[2]Stanford Applied Nanophotonics Laboratory, Stanford University, Stanford, CA 94305
tammyc@stanford.edu, jonfan@stanford.edu, tomlee@ee.stanford.edu

***Abstract*—Epidermal electronic systems, which conformally adhere to human skin, are a promising technology for wearable biomedical applications. Within these systems, the wireless components are made stretchable by translating solid traces into serpentine mesh patterns, which enable lateral spring-like mechanics. To ensure robust performance, there is a need to further study the impact of the serpentine mesh geometry and its stretching mechanics on microwave propagation. In this paper, we evaluate these impacts by modeling serpentine mesh traces in a microstrip system and extracting the corresponding effective transmission line parameters. The parameters are extracted by fitting full-wave results to an equivalent transmission line model. By demonstrating how the serpentine geometry and mechanics affect the power attenuation, electrical length, and impedance of microwave components, we provide a crucial step forward in the development of high-performance wireless wearable electronics.**

***Index Terms*—biomedical communication, flexible electronics, parameter extraction, transmission lines, wearable sensors.**

I. Introduction

In recent years, epidermal electronic systems have been developed for wearable biomedical applications such as physiological monitoring, wound treatment, biological sensing, and interfacing with implanted devices [1], [2]. These systems are stretchable, conforming to the mechanically soft epidermis for maximum comfort, high sensing precision, and optimal interfacing with implanted devices.

To operate autonomously, epidermal systems must transmit physiological information wirelessly and support wireless powering, typically at microwave frequencies. Thus, these systems have contained microwave interconnects, matching networks, and antennas [1]–[3]. These components are made stretchable by converting solid traces into serpentine mesh patterns capable of lateral spring-like mechanics. This conversion strategy is shown in Fig. 1, where the meshed lines become progressively stretchable as the curvature of the metal traces increases, denoted by the arc angle θ_{arc}. When the serpentine traces are bonded to an elastomer substrate, a stretchable microwave component is produced. As an example, we show an antenna consisting of concentric rings of serpentine traces undergoing stretching in Fig. 2. We have characterized this device for wireless powering from the epidermis to an implanted device [2].

While the design approach of Fig. 1 enables stretching mechanics for conventional microwave components, the subwavelength microstructuring of the metal traces impacts surface current propagation at high frequencies [4]. Therefore, there is a need to further study the influence of the serpentine mesh interconnection on microwave characteristics, to avoid potential parasitic effects or impedance issues in epidermal electronic systems [5]. Apart from a capacitive-coupling model that is specific to a coupling-based multiband antenna design [6], limited prior work exists for stretchable serpentine modeling at microwave frequencies.

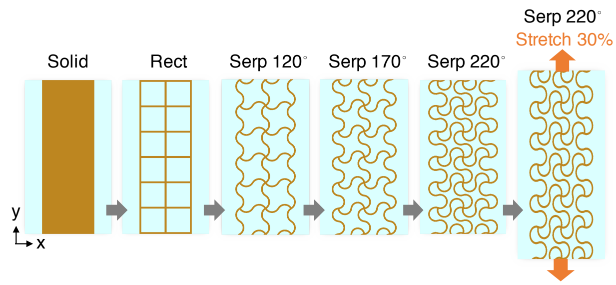

Fig. 1. Strategy for converting a rigid solid trace to a stretchable serpentine trace. *From left to right:* solid trace, rectangular mesh trace, serpentine mesh traces with arc angle $\theta_{\text{arc}} = 120°, 170°, 220°$, and serpentine mesh trace with $\theta_{\text{arc}} = 220°$ stretched by 30%.

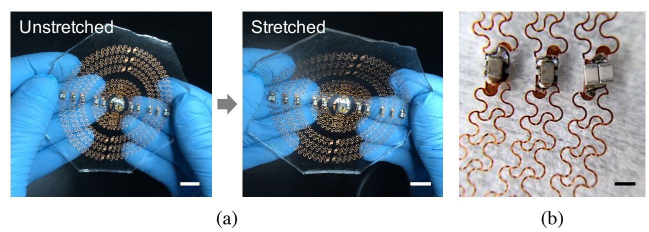

Fig. 2. (a) Stretchable antenna consisting of concentric serpentine traces for transmitting wireless power from the epidermis to an implanted device. Scale bars: 8 mm. (b) Close-up image of antenna, showing the serpentine traces with $\theta_{\text{arc}} = 175°$ and soldered 0805 components. Scale bar: 2 mm.

In this paper, we evaluate the impact of the serpentine mesh geometry and its stretching mechanics on microwave performance by extracting effective transmission line parameters for several conductive traces. Each trace in Fig. 1 is modeled above a dielectric elastomer substrate and conductive ground plane, forming a microstrip model. The effective characteristic impedance $Z_{0,\text{eff}}$ and propagation constant γ_{eff} are then extracted for each trace. In Section II, we describe the method used to extract the effective transmission line parameters. In Section III, this method is applied to the traces in Fig. 1 to evaluate the impact of the serpentine geometry as well as the impact of stretching on the microwave parameters. The extracted parameters are validated by comparing the predicted and full-wave S-parameters, and the significance of these results for wearable epidermal systems are discussed.

II. Method for Extracting Transmission Line Parameters from Stretchable Traces

To efficiently extract the transmission line parameters of the mesh traces in Fig. 1, we use a numerical method that selectively fits robust frequency points to an equivalent transmission line model. This approach was recently proposed for flexible PCBs with solid microstrip lines and meshed ground planes [7], and is applied here for stretchable epidermal systems with serpentine mesh lines. For this study, the mesh geometry is sufficiently sub-wavelength such that an equivalent transmission line model can be applied.

First, S-parameters are obtained from full-wave simulations and converted to ABCD-parameters. The peak points of the C-parameter are more robust to numerical error and are selectively fitted to the following equivalent transmission line model to obtain the per-unit-length impedance and admittance:

$$Z = R_0 + R_f\sqrt{f}(1+j) + j2\pi f L_{\text{pul}} \quad (1)$$
$$Y = G_0 + G_f f + j2\pi f C_{\text{pul}}. \quad (2)$$

Once the values of R_0, R_f, G_0, G_f, L_{pul}, and C_{pul} have been determined, the extracted effective propagation constant and characteristic impedance are given by:

$$Z_{0,\text{eff}} = \sqrt{\frac{Z}{Y}} \quad (3)$$
$$\gamma_{\text{eff}} = \alpha_{\text{eff}} + j\beta_{\text{eff}} = \sqrt{ZY} \quad (4)$$

where α_{eff} is the effective attenuation constant in Np/m and β_{eff} is the effective phase constant in rad/m.

To validate the extracted parameters, $Z_{0,\text{eff}}$ and γ_{eff} are used to predict the S-parameters for a given line length l and port impedance Z_0 according to the following relationship [8]:

$$S_{11} = \frac{(Z_{0,\text{eff}}^2 - Z_0^2)\sinh\gamma_{\text{eff}}l}{(Z_{0,\text{eff}}^2 + Z_0^2)\sinh\gamma_{\text{eff}}l + 2Z_0Z_{0,\text{eff}}\cosh\gamma_{\text{eff}}l}$$
$$S_{21} = \frac{2Z_0Z_{0,\text{eff}}}{(Z_{0,\text{eff}}^2 + Z_0^2)\sinh\gamma_{\text{eff}}l + 2Z_0Z_{0,\text{eff}}\cosh\gamma_{\text{eff}}l}.$$

The predicted S-parameters are then compared with the initial S-parameters from full-wave simulations of the stretchable serpentine traces to validate the extracted transmission line parameters.

III. Results and Validation

Each trace in Fig. 1 was simulated as a microstrip line in Ansoft HFSS. The mesh traces have a line width of 110 μm, a mesh spacing of 1.65 mm, and a thickness of 34 μm. The dielectric substrate is 1.35 mm thick PDMS ($\epsilon_r = 3$, $\tan\delta = 0.014$), a typical substrate for epidermal electronic systems. The line length is 13.16 mm.

The per-unit-length inductance L_{pul} and capacitance C_{pul} are determined from the simulated S-parameters for each line, and are shown in Table I. We see that L_{pul} increases from 263 to 481 nH as the solid line is converted to a serpentine mesh line of increasing arc angle. This increase is attributed to the narrow conductive traces that result from the meshing of the solid metal line, and to the increased winding of the traces as the arc angle increases.

TABLE I
Extracted Per-unit-length Inductance and Capacitance

Line Type	L_{pul} (nH)	C_{pul} (pF)
Solid	263	104
Rect	325	92
Serp 120°	366	94
Serp 170°	397	103
Serp 220°	481	114
Serp 220° (Stretch 30%)	448	104

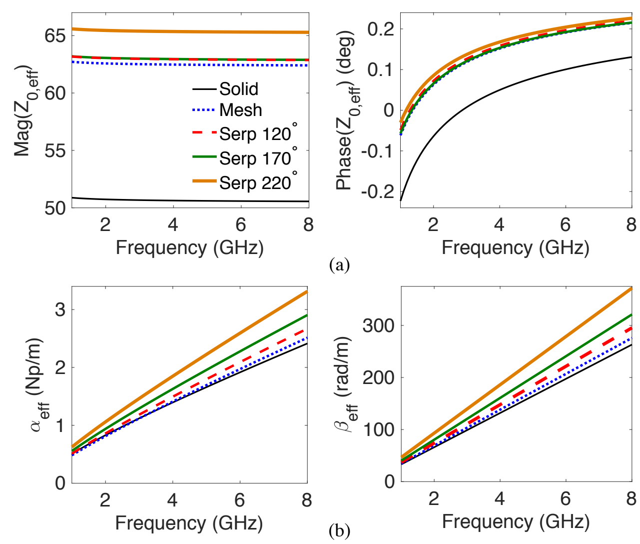

Fig. 3. The extracted (a) effective characteristic impedance $Z_{0,\text{eff}}$ and (b) effective propagation constant $\gamma_{\text{eff}} = \alpha_{\text{eff}} + j\beta_{\text{eff}}$ for solid, rectangular mesh, and serpentine mesh lines.

Similarly, C_{pul} changes during the conversion to a serpentine mesh, according to the amount of metal that composes the trace. When the solid line is first converted to a rectangular mesh, the area covered by trace metal decreases and C_{pul} correspondingly decreases from 104 to 92 pF. Then, as the curvature of the mesh traces increases, the area covered by the trace metal increases and, as a result, C_{pul} increases from 92 to 114 pF. Both L_{pul} and C_{pul} decrease with stretching as the serpentine unwinds and the amount of metal per-unit-length decreases.

The microwave propagation characteristics of epidermal systems correspond with these per-unit-length impedances, as described by Equations 1–4. Thus, in Fig. 3a, we see that the magnitude of the characteristic impedance $Z_{0,\text{eff}}$ increases from 51 to 65 Ω because of the conversion to a serpentine mesh line. This increase in characteristic impedance is significant and indicates that the overall dimensions of the serpentine mesh must be correctly scaled to avoid an unintended impedance mismatch within an epidermal electronic system.

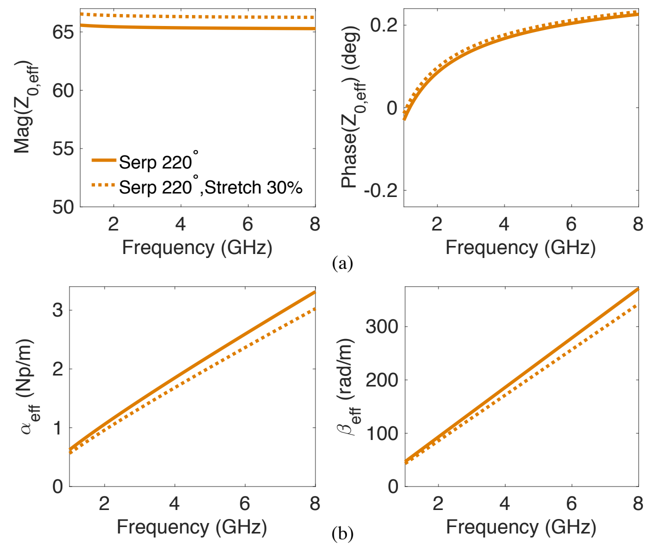

Fig. 4. The extracted (a) effective characteristic impedance $Z_{0,\text{eff}}$ and (b) effective propagation constant $\gamma_{\text{eff}} = \alpha_{\text{eff}} + j\beta_{\text{eff}}$ for serpentine mesh lines ($\theta_{\text{arc}} = 220°$), with and without 30% stretching.

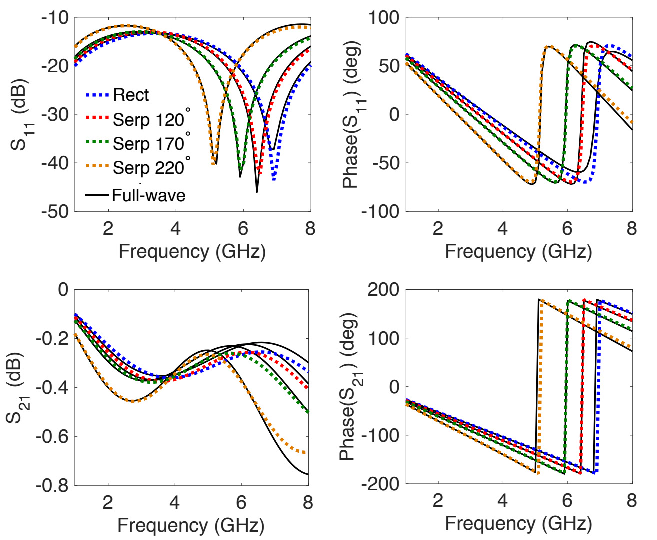

Fig. 5. Validation of extracted $Z_{0,\text{eff}}$ and γ_{eff} for rectangular and serpentine mesh lines. Predicted S-parameters using the extracted γ_{eff} and $Z_{0,\text{eff}}$ (colored, dotted) and S-parameters from full-wave simulations (black, solid).

Finally, the phase of $Z_{0,\text{eff}}$ undergoes a minor shift around 0.2° when the solid trace is meshed.

The plot for the effective propagation constant in Fig. 3b includes the attenuation and phase constants α_{eff} and β_{eff}, which provide information about the added loss and changes to electrical length as a result of the serpentine geometry. At 5 GHz, α_{eff} increases from 1.7 to 2.2 Np/m and β_{eff} increases from 165 to 233 rad/m as the modeled microstrip line is converted from solid to serpentine mesh. These increases in α_{eff} and β_{eff} are attributed to changes in trace length: when the arc angle increases, the winding of the traces grows and the cumulative trace length between consecutive vertices increases. Thus, the per-unit-length attenuation along the line increases, as surface current propagates along the narrow mesh traces and as coupling along the trace grows with increasing curvature. The increase in attenuation with increasing curvature indicates that in serpentine epidermal systems, there is an inherent trade-off between stretchability and microwave loss.

We also study how the stretching of epidermal electronic systems impacts microwave propagation, and the results are plotted in Fig. 4. Under an applied strain of 30%, the characteristic impedance is relatively constant, only increasingly marginally from 65 to 66 Ω. However, the attenuation and phase constants decrease with stretching from 2.2 to 2.0 Np/m and from 233 to 214 rad/m, respectively. The decrease in attenuation and electrical length is related to an unwinding effect in the serpentine mesh under stretching. Both the decrease in attenuation and in electrical length are advantageous and unique to the serpentine pattern, compared with composite material approaches for stretchable epidermal electronics. Of note is the decrease in phase constant; for resonant microwave devices, this effect allows the serpentine resonance to be more independent of stretching by counteracting the increase in physical length with a negative change in the phase constant.

Finally, we validate the extracted results for $Z_{0,\text{eff}}$ and γ_{eff} by comparing the predicted S-parameters with the S-parameters from full-wave simulation. As shown for the rectangular and serpentine mesh cases in Fig. 5, the predicted and full-wave values match closely.

IV. Conclusion

In this paper, we have demonstrated an efficient method for evaluating the microwave performance of wireless components in epidermal electronic systems. We show that the microwave attenuation due to the serpentine mesh geometry is offset by advantages in microwave performance under stretching. While our method has been used to evaluate serpentine mesh traces, it can be generally used to analyze various stretchable designs proposed for wearable systems. These results are crucial for improving the wireless performance of future wearable biomedical systems.

References

[1] D.-H. Kim, N. Lu, R. Ma *et al.*, "Epidermal Electronics," *Science*, vol. 333, no. 6044, pp. 838–844, Aug. 2011.

[2] T. Chang, Y. Tanabe, C. C. Wojcik *et al.*, "A General Strategy for Stretchable Microwave Antenna Systems using Serpentine Mesh Layouts," *Adv. Funct. Mater.*, vol. 27, no. 46, p. 1703059, Dec. 2017.

[3] X. Huang, Y. Liu, G. Kong *et al.*, "Epidermal radio frequency electronics for wireless power transfer," *Microsyst. & Nanoeng.*, vol. 2, p. 16052, Apr. 2016.

[4] T. Chang, C. Wojcik, Y. Su *et al.*, "Characterization of Stretchable Serpentine Microwave Devices for Wearable Electronics," *Proc. of IEEE MTT-S Int. Microw. Symp.*, Honolulu, HI, USA, Jun. 2017.

[5] Y.-S. Kim, J. Lu, B. Shih *et al.*, "Scalable Manufacturing of Solderable and Stretchable Physiologic Sensing Systems," *Adv. Mater.*, vol. 29, no. 39, Oct. 2017.

[6] S. I. Park, G. Shin, J. G. McCall *et al.*, "Stretchable multichannel antennas in soft wireless optoelectronic implants for optogenetics," *Proc. Natl. Acad. Sci. U.S.A.*, vol. 113, no. 50, pp. E8169–E8177, Nov. 2016.

[7] J. He, C. Hwang, J. Pan *et al.*, "Extracting the Characteristic Impedance of a Transmission Line Referenced to a Meshed Ground Plane," *Proc. of IEEE Int. Symp. on Electromagn. Compat.*, Ottawa, ON, Canada, Jul. 2016.

[8] P. A. Rizzi, *Microwave Engineering Passive Circuits*. Englewood Cliffs, NJ: Prentice Hall, 1988.